IMPACT OF HYDROCHLORIC ACID (HCL) TREATMENT ON DIATOMITE PURITY AND STRUCTURAL MODIFICATIONS FOR ADVANCED PHOTOVOLTAIC APPLICATIONS

A. ZEBOUDJ[1,*], S. HAMZAOUI[1], M. ZEBOUDJ[2], M. ADNANE[1], L. LEONTIE[3], S. GURLUI[3], A. CARLESCU[4]

[1] LMESM Laboratory, Physics Department, University of Science and Technology Mohamed Boudiaf (USTO-MB) Oran 31000, Algeria
[2] SIMPA Laboratory, Computer Science Department, University of Science and Technology Mohamed Boudiaf (USTO-MB) Oran 31000, Algeria
[*]*Corresponding author, Email: asmaa.zeboudj@univ-usto.dz*
[3] Faculty of Physics, Alexandru Ioan Cuza University of Iasi, Bulevardul Carol I, Nr. 11, 700506 Iasi, Romania
[4] Science Research Department, Institute of Interdisciplinary Research, Research Center in Environmental Sciences for the North-Eastern Romanian Region (CERNESIM), Alexandru Ioan Cuza University of Iasi, 11 Carol I, 700506 Iasi, Romania

Received November 10, 2024

Abstract. Our work focused to prepare diatomite-silica that can be reduced to silicon, Algerian diatomite was synthesized through a chemical method. This research aimed to study the influence of acid treatment and grinding on diatomite's impurity level. An analysis of the X-ray photoelectron spectroscopy (XPS) showed a decrease in the concentration of impurities in the diatomite.

A hydrochloric acid (HCl) concentration that's 4 mol/L resulted into a soft leaching of most organics such as carbon, but still retained impurities. The X-ray diffraction (XRD) analysis also confirmed that the chemical configuration of SiO_2 was barely altered. In comparison, grinding led to an invasion of diatomite by impurities and to structural disorders. These findings are relevant for encouraging work on purification steps which facilitate the extraction of non-pertaining silica while producing solar silicon for solar cells.

Key words: Silicon, silica, X-ray photoelectron spectroscopy (XPS), photovoltaic cells, the purity, HCl.

DOI: https://doi.org/10.59277/RomJPhys.2025.70.608

1. INTRODUCTION

Silicon (Si), a relatively common element on the Earth's crust [1], occurs in nature mainly as silicon dioxide at silica [2]. It is an important component in the electronics industries, particularly in photovoltaic cells and semiconductor devices [3] that is abundant and exhibits interesting electrical characteristics [4]. In order to achieve the desired performance requirements, it is necessary to use high-purity silicon [5], which can be obtained, from the quarries with natural silica like, quartz, sand or diatomite [6].

However, silica is starting substance of the formation of many classes of materials such as polymers, ceramics and semiconductors [7, 8]; it is also used in many domains as pharmacy application for example therapeutic, biochemistry and biomedicine [9, 10].

The first stage of the silica purification process involves the crushing and washing processes [11], which are aimed at removing coarse impurities and preparing the silica for subsequent chemical purification, when metal and nonmetal impurities are eliminated at the molecular level [12]. A significant amount of time and energy is spent on this purification procedure in order to obtain pure silicon by the reduction of silica [13]. Recently, new approaches to silica reduction have been proposed including novel electrochemical methods termed carbothermic reduction [14, 15] as well as many others. The latter process involves the heating of silica (SiO_2) along with carbon which is a reducing agent in a high-temperature about (1700–2000°C) [16] electric furnace. The reaction leads to the production of metallurgical silicon and carbon monoxide (CO) gas which is quite harmful [17].

However, the silicon obtain contains metallic impurities likes, iron, aluminum, calcium and carbon residues [18], making the purity insufficient for some applications. In addition, this process is expensive and requires a large amount of electrical energy [19].

To overcome these limitations, an alternative is to produce silicon by purifying silica from diatomaceous earth by chemical attack. This study explores the effect of hydrochloric acid (HCl) treatment on diatomaceous earth, which could constitute a stable and alternative source of silica for the photovoltaic industry [20], in particular thanks to the simplicity of the proposed purification process.

2. EXPERIMENTAL

A diatom from north of Algeria (Fig. 1) suffered in the first mechanically crushed using a grinder, for 30 minutes in order to refine the particle size. Following this; A solution with 20 g of diatomaceous powder was prepared by mixer 4 mol/L hydrochloric acid (HCl); which was then heat to 150°C for 2 hours. After that, an acid leaching performed, rinse with distilled water use a centrifuge until found neutral pH (pH = 7). This process is described by the following chemical reaction [21]:

$$SiO_2 + 4HCl \rightarrow SiCl_4 + 2H_2O. \quad (1)$$

In this reaction, silicon dioxide (SiO_2) reacts with hydrochloric acid (HCl) to form water (H_2O) and silicon tetrachloride ($SiCl_4$). Initially, an H^+ ions from hydrochloric acid reacts with silicon dioxide, resulting in hydrated silicon dioxide [20, 21]. This intermediate compound is unstable and converts into silicon tetrachloride ($SiCl_4$) and water. Therefore, silicon tetrachloride ($SiCl_4$) is the primary product of this reaction.

Fig. 1 – Diatomaceous earth presentation.

X-ray photoemission spectroscopy and X-ray diffraction was resorted to establish the purity and quality of the silica before and after chemical refinement.

X-ray photoelectron spectroscopy XPS was carried out using a monochromatic aluminum K alpha (1486.6 eV) micro-focus with variable spot sizes ranging from 30–400 μm. Hemispheric analyzer and multi-channel detectors were utilized for the study, this process was made at ultra-high vacuum chambers of about 10^{-9} mbar by utilizing turbo molecular and ion pumps linked to a computer with diagnostic software. The data result presents the intensity plotted against binding energy. The number of peaks in the spectrum corresponds to the number of atomic orbitals of chemical elements lying on the surface of the specimen out to specific electrons and the allowable area of each peak is a coefficient of concentration of the element. This method makes it possible to study the state of the surface of silica, including the state after pulverization as well as without it.

The X-ray diffraction XRD characterization was done with a Shimadzu LabX XRD-6000 diffractometer using copper K(alpha) radiation (λ = 1.54059 Å). The diffraction patterns were obtained within the 2θ range 20º –80º at a step size of 0.05º and a rate of scanning of 4 deg/minute.

3. RESULTS AND DISCUSSION

The X-ray diffraction XRD patterns were studied using X'Pert High Score program with a 2016 database (Fig. 2).

Figure 2 illustrates peaks designated with Miller indices such as (011), (110), (111), (012), and (202) which indicate various orientations of the crystal structures in the material. In the sample without HCL (raw sample) treatment, the most intense peaks show up at 9°, 21° and 26°, approximately. There are features of iron and silicon at peaks roughly 2θ = 28°, 47° and 56° and another pic of aluminum-silicon between 40° and 60°.

In the raw sample, the peak intensities are fairly low, the principal peak (011), associated with silicon, reached a maximum of only about 1000 units near 2θ = 26.6°. This peak is invariably found in both the treated and untreated samples confirming quartz to be present in both types of diatomite.

The peaks at 9°, 21°, 26°and 28° gradually become visible after the sample was treated with HCl acid along with an additional peak at 2θ = 47° that due to silicate phase which is formed because of the acid treatment. In this treated sample the peak intensities are very much higher with the principal peak (011) attaining over 2000 units. This increase in intensity indicates that the acid treatment has in fact resulted in the removal of iron oxides and aluminum oxides impurities which have covered parts of the crystalline structure.

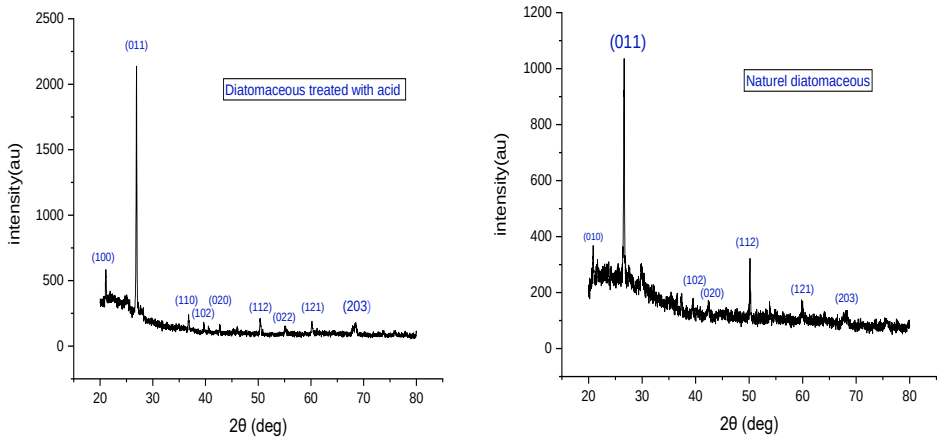

Fig. 2 – XRD analyze of diatomite from north of Algeria.

X-ray Photoelectron Spectroscopy (XPS) analysis patterns studied for both raw diatomite and acid-treated diatomite present in Fig. 3 and Fig. 4.

Figures 3 present the spectra named respectively Wide Spectrum to identify the surface elements of the sample and their chemical states during X-ray photoelectron spectroscopy (XPS) analysis. Spectrum (a) is used for the first analysis of raw diatomite, while Spectrum (b) analyzes diatomite after the sputtering process, where the sample was prepared by removing a surface layer through ion bombardment to clean the surface and analyze the composition of the subsurface layers. Both spectra show peaks at binding energies specific to electrons in given sample atoms.

These binding energies are provided for elements in various orbitals, with their intensity measured in arbitrary units (a.u). This means that the intensity measures the quantity of electrons observed for each binding energy. The elements in the material are identified by four differents peaks corresponding to the following elements: Silicon (Si 2p), Oxygen (O 1s), Carbon (C 1s), and Nitrogen (N 1s).

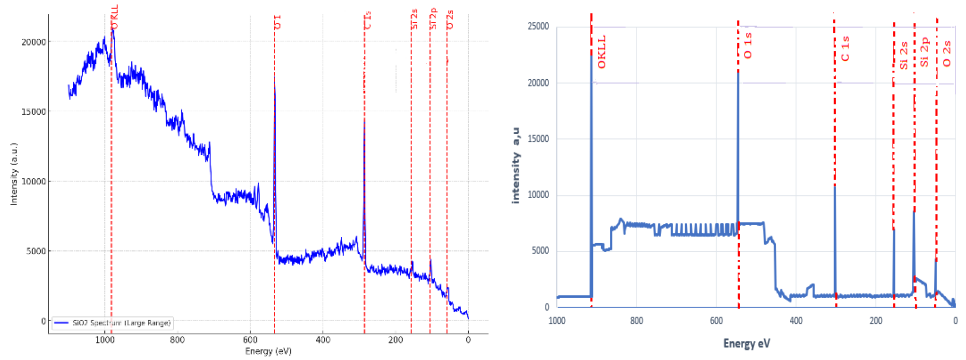

(a) (b)

Fig. 3 – Spectrum of raw diatomite before (a) and after (b) the sputtering process.

In the case of Spectrum (a), we identify, Carbon Peaks between 286 eV and 290 eV, typically associated with C-C or C-H. has energy of 286 eV C-C or C-H bond peak. Peaks between 288.2 eV and 289.5 eV correspond to drinks and the carbon Indicator of oxygen C = O. These peaks indicate organic residues, probably biological material or contaminants. Oxygen peaks (O 1s) are observed around 530–540 eV with a binding energy of 529.5–530.5 eV, typically associated with oxygen in metal oxides, between 531-532 eV oxygen is bonded to carbon (C=O).

The peaks between 532.5, 536.8 eV include different possible states of the O hydroxyl followed by the peaks between 537.3 and 539.8 eV seem related to less common states. Finally, between 540.1 eV and 543.0 eV, these peaks could indicate adsorbed oxygen or contaminants on the surface, thus indicating a SiO_2 majority of the surface.

Then we notice peaks between 100–105 eV of silicon (Si 2p). The peak at 102.5 eV, we can then say that this is in agreement with the silicon in SiO_2 other peaks between 103.0 eV and 103.2 eV then link well to the binding energies of the silicon in the oxide of silicon SiO_2. This confirms the presence of SiO_2, typical of diatom frustules in the analyzed sample, and lastly, we find for Energy around 395–405 eV a nitrogen peak (N 1s) corresponding to the bond (N-C or N-O) which indicate residues of proteins or other biomolecules.

The second spectrum (b) presents peaks as follows, one of them is KLL peak with 982 eV energy corresponding to oxygen which confirms its presence in the sample by a KLL Auger transition, another one is for oxygen O 1s at 533 eV, the oxidizing compounds such as SiO_2 and also there is a peak of O 2s which typically shows some more amount of oxygen.

In addition, other peaks include carbon, C 1s at 284 eV that generally arise from surface impurities but could also be attributed to residual organics. Finally, the silicon states are well described by Si 2s and Si 2p peaks at approximately 157 and 105 eV respectively.

Clearly defined significant peaks for oxygen (O KLL, O 1s, O 2s) and silicon (Si 2s, Si 2p) suggest that the sample mostly consists of SiO_2. Low levels of carbon (C1) can be an indication of slight contamination usually resulting from environmental hydrocarbons or process residues.

3.1. CALCULATION OF ATOMIC CONCENTRATION

From these spectra, the atomic concentration of each element can be determined by normalizing the areas under the peaks, corrected by the atomic sensitivity factors (ASF) specific to each element. The atomic concentration proportional to the area under the curve of the different peaks, is recorded in Tables 1 and 2.

Table 1

The atomic concentration of each element in diatomite without sputtering

Element	Area (eV)	Corrected Area (eV)	ASF	Atomic Concentration (%)
O 1s	30983.6	68339.1	0.71	37.20
C 1s	29788.3	23718.4	1.00	29.70
Si 2p	4964.1	7482.2	0.81	5.40
N 1s	14112.1	29631.2	0.47	27.60

Table 2

The atomic concentration of each element in diatomite after sputtering

Element	Area (eV)	Corrected Area (eV)	ASF	Atomic Concentration (%)
O 1s	48652.3	68456.1	0.71	38.80
C 1s	22052.8	22052.8	1.00	24.80
Si 2p	9267.7	10654.0	0.81	9.70
N 1s	14001.4	29373.2	0.47	26.60

Quantitative analysis for a raw sample before and after sputtering is presented in Tables 1 and 2 from data on different parameters, it seen that oxygen concentration relatively maintains its stability upon sputtering with minimal boost from 37.20% to 38.20%. There was also noted a drop in carbon content following sputter coating which has led to decrease of their percentage from 29.70% to 24.80%. The decline observed might suggest a possible removal of carbon-based contaminations present on the surface of the sample material.

Moreover, after sputtering silicon concentration increases, the percentage rises from 5.40% to 9.70%. In the end, nitrogen concentration remains relatively constant with a minor decrease from 27.60% to 26.60%.

Comparison of results from both tables reveals that carbon concentration was mostly affected by sputtering as it was intended for cleaning sample surface and hence eliminating impurities on it. Furthermore, the presence of higher levels of silicon also shows that layers beneath contained more silicon in them. Oxygen and nitrogen concentrations remain stable there by indicating homogeneity in these elements' distribution in the near surface and sub-surface layers of the sample.

The results of diatoms chemically treated with hydrochloric acid (HCl), as observed in the XPS data, are represented by spectra (a) and (b) (Fig. 4). The first step in the analysis of treated diatoms chemically with HCl corresponds to spectrum (a). Subsequently, spectrum (b) reveals further analyzes of diatoms chemically treated with hydrochloric acid (HCl) and having undergone a sputtering process.

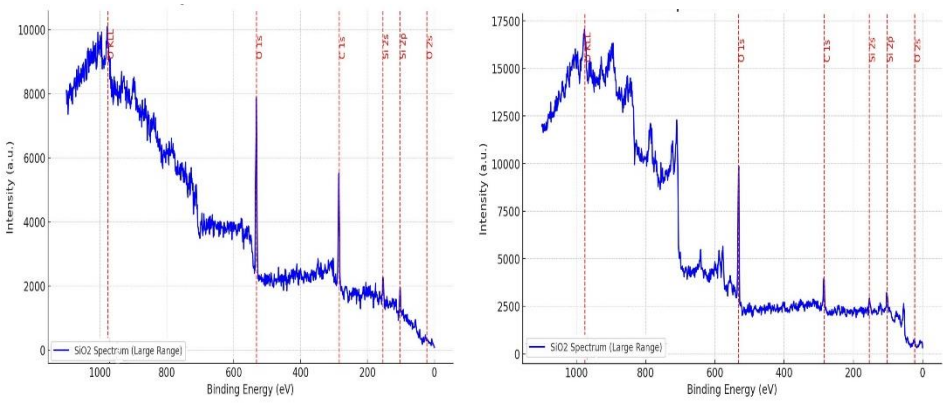

Fig. 4 – Spectrum of diatoms chemically treated with hydrochloric acid before (a) and after (b) the sputtering process.

According to the analysis of the first spectrum (a), we could identify several peaks. The carbon peaks (C 1s) generally appear around 284.8 eV for C-C and C-H bonds, while the C-O bond has an energy of 286 eV and 288.5 eV for C=O bonds. The presence of these peaks suggests damage to the surface, likely caused by organic residues resulting from biological matter or other contaminating substances. Particularly strong peaks of oxygen (O 1s) are observed around the value of 532 eV which is for silicon oxide and 533 eV for hydroxyl groups (OH) and adsorbed water (H_2O). The peaks corresponding to silicon (Si 2p and Si 2s) appear around 103.3 eV and 154.0 eV. These peaks reveal a moderate intensity indicating the presence of SiO_2, which is characteristic of diatom frustules. Finally, the presence of chlorides (Cl 2p) is indicated by the peak observed at 198 and 202 eV, which results from the treatment of diatoms with HCl.

In the XPS spectrum of the sputtering SiO_2 present in (b), it is possible to distinguish several energy peaks ranging from 0 eV to 1000 eV including: Oxygen

peak (O 1s) around 532 eV and an intensity very high, which confirms the majority composition in SiO_2 and shows a significant quantity of oxygen. Peak (O 2s) at 23 eV and of a relatively low intensity, indicating the presence of oxygen in another type of bond, which generally corresponds to the state bound to a metal, such as silicon. Carbon C 1s peak around 285 eV less intense. This peak is probably due to contamination of the sample surface by organic residues present in the environment or in the samples. The peaks Si 2p, Si 2s at 103 eV and 154 eV respectively with moderate intensity confirming the presence of silicon in the oxidized state.

The XPS spectra of HCl treated SiO_2 before and after the sputtering show similar compositions in terms of major observed peaks. This suggests that sputtering did not significantly change the oxygen and silicon content at the surface of the sample. The carbon contamination is however depicted in both spectra, yet an additional oxygen peak after deposition indicates another metal bound oxygen configuration which can be due to the spraying process.

Our findings show a distinct decrease in C 1s peaks indicating a notable reduction in organic impurities situated on the surface of diatoms. Such information is vital for enhancing their utilization in various scientific and industrial applications. On the other hand, insignificant changes in Si 2p peaks before and after treatment indicate that HCl does not significantly affect the chemical structure of SiO_2. The presence of hydroxyl groups coupled with overall stability demonstrates that diatoms retain their hydrophilic and structural attributes which are essential for biomimetic and environmental purposes.

The results of diatoms before and after HCl treatment of our experiment align with observations from related research, a study by Hiroshi Okada and Masatoshi Shinohara [21] on HCl-treated GaN surfaces also revealed a significant reduction in surface oxides, indicating HCl's effectiveness in cleaning surfaces without altering the core chemical structure. Similarly, research by Matthew Nooney and Vladimir Liberman [22] on GaAs surface treatments showed that HCl could remove oxides and enhance electrical properties while preserving the underlying structure. In contrast, a study by Wulan and Ulwani [23] on HCl-treated carbon nanotubes found that although HCl treatment improves nanotube dispersion, it may introduce structural irregularities and impurities, like to those seen in our sputtered samples. This consistency across studies reinforces our findings and highlights a broader trend in this area of research.

4. CONCLUSION

A deep and nuanced understanding of the chemical composition and surface modifications of diatoms before and after HCl treatment is revealed in XPS and XRD analysis results. Based on our experimental data, it can be concluded that the treatment with HCl has a significant effect on the surface properties of the studied

diatoms, improvements in purity, crystallinity and increases in the volume fraction of quartz of the diatomite. This is evidenced by increased intensity of the peaks, decreased width of the peaks, and better structural stability of silica. The structural improvements will contribute towards making the sample cleaner, and may allow for better industrial or scientific applications that depend on silica of high quality.

Comparing XPS spectra before and after sputtering, it can be seen clearly that contaminants have reduced significantly peaks are more pronounced while background noise is reduced. Peaks for Si and O elements in interest are more distinct and well defined after sputtering, the sputtered samples are purer than those unsputtered for SiO_2 indicating the efficiency of chemical purification process. This is supported by the decrease in the peaks associated with carbon impurity.

Acknowledgements. We would like to express our gratitude to the LMESM Laboratory, Physics Department, University of Science and Technology Mohamed Boudiaf, for their support and resources. Additionally, we extend our thanks to the Physics Laboratory, Physics Department, Alexandru Ioan Cuza University, Iași, Romania, for providing the opportunity for an internship and for their advanced instrumentation.

REFERENCES

1. I. Slatni, F. Z. Elberrichi, J. Duplay, N. E. H. Fardjaoui, A. Guendouzi, O. Guendouzi, B. Gasmi, F. Akbal and I. Rekkab, *Mesoporous silica synthesized from natural local kaolin as an effective adsorbent for removing acid red 337 and its application in the treatment of real industrial textile effluent*, Environ. Sci. Pollut. Res. Int. **27**(31), 38422–38433 (2020).
2. A. Sharma and D. Penumadu, *Role of particle shape in determining tensile strength and energy release in diametrical compression of natural silica grains*, J. Mater. Sci. **60**(5), 1299–1311 (2020).
3. D. J. Rosenberg, S. Alayoglu, R. Kostecki and M. Ahmed, *Synthesis of microporous silica nanoparticles to study water phase transitions by vibrational spectroscopy*, Nanoscale Adv. **1**, 4878–4887 (2019).
4. P. Curnow, L. Senior, M. J. Knight, K. Thamatrakoln, M. Hildebrand and P. J. Boothet, *Expression, purification, and reconstitution of a diatom silicon transporter*, Biochemistry **51**, 3776–3785 (2012).
5. B. Das, T. K. Mandal and S. Patra, *Biodegradation of phenol by a novel diatom BD1IITG – kinetics and biochemical studies*, Int. J. Environ. Sci. Technol. **13**, 529–542 (2016).
6. K. Ifuku, D.Yan, M. Miyahara, N. Inoue-Kashino, Y. Y. Yamamoto and Y. Kashino, *A stable and efficient nuclear transformation system for the diatom Chaetoceros gracilis*, Photosynth. Res. **123**, 203–211 (2015).
7. Dorfner Anzaplan, *Evaluation of High Purity Resources (I)*, Laboratory Analyses. Brochure, 2013.
8. A. Sdiri, T. Higashi, S. Bouaziz and M. Benzina, *Synthesis and characterization of silica gel from siliceous sands of southern Tunisia*, Arab J. Chem. **7**, 486–493 (2014).
9. E. V. Armbrust, J. A. Berges, C. Bowler, B. R. Green, D. Martinez et al., *The genome of the diatom Thalassiosira pseudonana: ecology, evolution, and metabolism*, Science **306**, 79–86 (2004).
10. M. S. Aw, S. Simovic, J. Addai-Mensa and D. Losic, *Silica microcapsules from diatoms as new carrier for delivery of therapeutics*, Nanomedicine **6**, 1159–1173 (2011).
11. C. Bowler, A. Allen, J. Badger et al., *The Phaeodactylum genome reveals the evolutionary history of diatom genomes*, Nature **456**, 239–244 (2008).

12. S. Chandrasekaran M. J. Sweetman, K. Kant, W. Skinner et al., *Silicon diatom frustules as nanostructured photoelectrodes*, Chem. Commun. **50**, 10441–10444 (2014).
13. H. Chtourou, I. Dahmen, A. Jebali, F. Karray et al., *Characterization of Amphora sp., a newly isolated diatom wild strain, potentially usable for biodiesel production*, Bioprocess Biosyst. Eng. **38**, 1381–1392 (2015).
14. S. R. Cicco D. Vona, E. De Giglio, S. Cometa, M. Mattioli-Belmonte et al., *Chemically modified diatoms biosilica for bone cell growth with combined drug-delivery and antioxidant properties*, Chem. Plus. Chem. **80**, 1104–1112 (2015).
15. Y. Carvalho, J. M. A. R. Almeida, P. N. Romanot et al., *Nanosilicalites as support for β-glucosidases covalent immobilization*, Appl. Biochem. Biotechnol. **182**(4), 1619–1629 (2017).
16. R. Thahir, A. Wahab, W. Taba et al., *Synthesis of mesoporous silica SBA-15*, Rasayan Journal of Chemistry **12**(3), 1117–1126 (2019).
17. A. Zeboudj, S. Hamzaoui, *Extraction of silica from natural deposits for the production of silicon in photovoltaic applications*, Open J. Bac. **7**(1), 011–015 (2023).
18. Y. Mochizuki, J. Bud, J. Liu and N. Tsubouchi, *Production of silicone tetrachloride from rice husk by chlorination and performance of mercury adsorption from aqueous solution of the chlorinated residue*, ACS Omega **5**(45), 29110–29120 (2020).
19. P. Gentile, A. Solanki, N. Pauc, F. Oehler et al., *Influence of HCl on doping and morphology control in silicon nanowires*, Nanotechnology **23**(21), 215702 (2012).
20. H. Lefler, Y. Zhang, Z.Z Fang et al., *Removal of silicon from highly acidic HCl medium to produce purified TiO_2*, Hydrometallurgy **173**, 218–223 (2017).
21. N. Matthew, L. Vladimir, X. Mingde et al., *Reaction of HCl with the GaAs (100) surface*, Surface Science **302**(1–2), 192–204 (1994).
22. H. Okada, M. Shinohara, Y. Kondo et al., *Investigation of HCl-based surface treatment for GaN devices*, AIP Conf. Proc. **1709**, 020011 (2016).
23. P. Wulan, P. D. K. Ulwani et al., *The effect of hydrochloric acid addition to increase carbon nanotubes dispersibility as drug delivery system by covalent functionalization*, IOP Conf. Ser.: Mater. Sci. Eng. **316**, 012013 (2018).